WP15ER-CPR(17) 17306

M Chernyshova et al.

Application of GEM Based Detector Measurements for Plasma Impurity Radiation Monitoring: Laboratory Tests

Preprint of Paper to be submitted for publication in Proceeding of 13th International Symposium on Fusion Nuclear Technology (ISFNT)

This work has been carried out within the framework of the EUROfusion Consortium and has received funding from the Euratom research and training programme 2014-2018 under grant agreement No 633053. The views and opinions expressed herein do not necessarily reflect those of the European Commission.

Performance of Gas Electron Multiplier based detector aimed at plasma impurity radiation monitoring

Maryna Chernyshova[a], Karol Malinowski[a], Yevgen Melikhov[b], Ewa Kowalska-Strzęciwilk[a], Tomasz Czarski[a], Andrzej Wojeński[c], Paweł Linczuk[a,c], Rafał D. Krawczyk[c]

[a]*Institute of Plasma Physics and Laser Microfusion, Hery 23, 01-497 Warsaw, Poland*
[b]*School of Engineering, Cardiff University, CF24 3AA, Cardiff, U.K.*
[c]*Warsaw University of Technology, Institute of Electronic Systems, Nowowiejska 15/19, 00-665 Warsaw, Poland*

For the purpose of monitoring the level of impurity (especially tungsten) and its distribution reconstruction at tokamaks (ITER in particular), a Soft X-Ray (SXR) tomographic diagnostics based on Gas Electron Multiplier (GEM) detectors with energy discrimination has been extensively considered for a while. Coupled with advanced electronics, GEM detectors offer excellent time and space resolution, as well as a charge spectrum from which the SXR photon spectrum can be deconvolved. In addition, they are less subjected to a neutron damage as compared to standard semiconductor diodes. This contribution highlights the latest studies supporting the development of such diagnostics focusing on laboratory tests to examine: (a) the impact of GEM holes geometry on the properties and distribution of the electron avalanche; (b) the effect of the high rate photon flux on GEM foil performance; and (c) the optimal electric field distribution.

Keywords: Nuclear instruments for hot plasma diagnostics, X-ray detectors, Electron multipliers (gas), Micropattern gaseous detectors (MSGC, GEM, THGEM, RETHGEM, MHSP, MICROPIC, MICROMEGAS, InGrid, etc.).

1. Introduction

Tungsten has been the main candidate for the plasma facing material in ITER and future fusion reactor for some time forced a creation of the ITER-oriented research programs to effectively monitor the impurity level of tungsten in plasma. For this purpose, the detection system based on Gas Electron Multiplier (GEM) technology [1], [2] has been recently proposed as a Soft X-Ray tomographic system and is being continuously developed by our group [3], [4], [5], [6]. Detectors built based on this technology are expected to satisfy the main constraints on dimension, spatial position and required energy sensitiveness imposed on any X-ray detector for tokamak plasma in ITER and/or DEMO. A detecting system, based on two GEM detectors with planar and cylindrical geometry would allow performing poloidal tomography, i.e. an ultimate goal to be implemented for plasma impurities transport studies. Such a system has been designed, modelled, and laboratory and tokamak tested through collaboration between IPPLM, WUT, and CEA [7], [8], [9], [10], [11], [12]. It is to be installed in a poloidal section of the WEST project tokamak and are going to be put inside the vertical and outside the horizontal ports, respectively [5], [13], [14].

This work is focused on tests supporting the design of the internal structure of the detector and optimization of its performance: (a) the impact of GEM holes geometry on the properties and distribution of the electron avalanche; (b) the effect of the high rate photon flux on GEM foil performance; and (c) the optimal electric field distribution.

2. Detector performance optimization tests

2.1 Experimental setup and methods

The principle of the GEM detector operation is based on the collection of electrons induced by photoabsorption of the incident photons with energy $h\nu$ passing through the detector window. The released photoelectrons of energy $\varepsilon = h\nu - \varepsilon_b$, where ε_b is the electron binding energy, ionize the neighboring gas atoms producing primary ion-electron pairs. The binding energy could be liberated either by emission of Auger electron resulting in creation of the created electron-ion pairs, or by K-series X-ray fluorescence of energy $\approx 2.9\ keV$. The latter could escape the detection volume leading to a satellite line in the observed spectrum for incident radiation energy higher 3.2 keV, the Ar K-edge. The average number of primary ion-electron pairs can be evaluated as ε / w_I, where w_I is the average energy per ion-electron production which varies between 20 eV and 40 eV for most gases, and is $\approx 27\ eV$ for Ar/CO_2.

In the detector, the primary electron cloud that was created in the so-called drift gap, is subject to a moderate electric field that forces the cloud to move towards a GEM foil. An electric field of 50-100 kV/cm in the holes of the GEM foil is high enough to cause multiple secondary ionizations of the gas. This initiates an electron avalanche generation. In case of the detector with two/three foils, the avalanche is then moved through transfer gap(s) with a moderate electric field and through another GEM foil(s) experiencing further amplification. After the last GEM foil, this avalanche is injected into the final segment of the detector, a so-called induction gap, and is collected on the patterned readout/anode plane. In this way, the induced anode current signals are detected by electronics. At the

author's email: maryna.chernyshova@ipplm.pl

proper conditions, three GEM foils powered by high voltage would result in primary electrons multiplication of $10^3 - 10^5$ times.

The detector used in this work is a standard triple GEM detector of 5/2/2/2 mm spacing filled with Ar/CO_2 $70/30$ mixture at up to 70 ml/min flow rate. The 50 µm thick GEM foils used for these measurements were either double-conically (70/50 µm outer/inner diameter holes, 140 µm pitch, hexagonal arrangement) or cylindrically (70 µm diameter holes, 140 µm pitch, hexagonal arrangement) shaped. The readout pixel structure (anode) was connected to pico-ammeter (Keithley 6487) through the 100 $k\Omega$ protecting resistor. In addition to the anode signal, the signal from the bottom electrode of the last GEM foil was collected using the following arrangement: the electrode, decoupling capacitor of 2.2 nF, charge preamplifier (ORTEC 142), shaper (ORTEC 450), and finally a Multi-Channel Analyzer (AMPTEK 8000D). Two sources of photons were used to test the performance of the detector: (a) a collimated ø1.2 mm beam of 8 keV photons from a copper X-ray generator of 1kHz-1MHz intensity, and (b) 2kHz intense ^{55}Fe source. Before start of the each measurement, enough time was allowed to stabilize for charging up effect.

Ultimately, the effective electron gain, i.e. number of electrons that have reached the readout plane, was estimated as $G_{eff} = \frac{I_{anode}}{e \cdot N \cdot Rate}$, where I_{anode} is the anode current, N is the number of primary electrons, $Rate$ is the measured photon rate and e is the electron's charge. The energy resolution of the detector was evaluated as $\sigma E/E$ ratio of the 5.9 keV peak for ^{55}Fe pulse-height distribution.

In order to be able to compare the performance of two detectors with different holes geometries, each GEM foil voltage was kept at 380 V. This selection made sure that the observed changes are related to the holes geometry, to external electric fields around the foils (adjusted by voltages at drift, two transfer, and induction gaps) and/or to photon flux value.

2.2 Gain vs. electric field distributions

Initially, a drift voltage scan was performed for 0-1500 V values to select the "plateau" region of maximal charge collected. It was turned to be within the region of about 300-800 V. Thus, three drift voltages were considered for further tests: $U_{drift} = 300, 500, 700\, V$. Both first and second transfer voltages were chosen in the range of $U_{T1,T2} = 300{:}\,150{:}\,900\, V$, and the induction gap voltage was in the range of $U_{Ind} = 600{:}\,100{:}\,1000\, V$. Since the used GEM detector is an open gas system, pressure dependent characteristics had to be taken into account: the data were normalized to incorporate the changes caused by weather conditions.

The effective electron gain is directly proportional to these three major factors: the gas gain, and the collection and extraction efficiencies. The gas gain sets the number of secondary electrons produced in a GEM hole from one incoming electron. It could be written as $\bar{G} = \exp\left(\int \alpha(\vec{E})dr\right)$, where α is the first Townsend coefficient dependent on electric field $\vec{E}$, pressure and gas type (here the following contributions were neglected: space charge influence, electron attachment and photoelectron emission). The collection efficiency defines the number of electrons brought to the GEM hole. It is a function of electric fields above and inside the hole as trajectories of electrons are influenced by field lines. The same can be said about the extraction efficiency, i.e. the number of electrons extracted from the GEM hole: it is a function of electric fields inside and below the hole. An interplay between all electric fields existing in the triple GEM detector governs the effective electron gain in a complex way as opposed to the much simpler case of a single GEM detector [15], [16]. In this work, the effective electron gain was examined to find an optimal electric field distribution for which the gain is maximized.

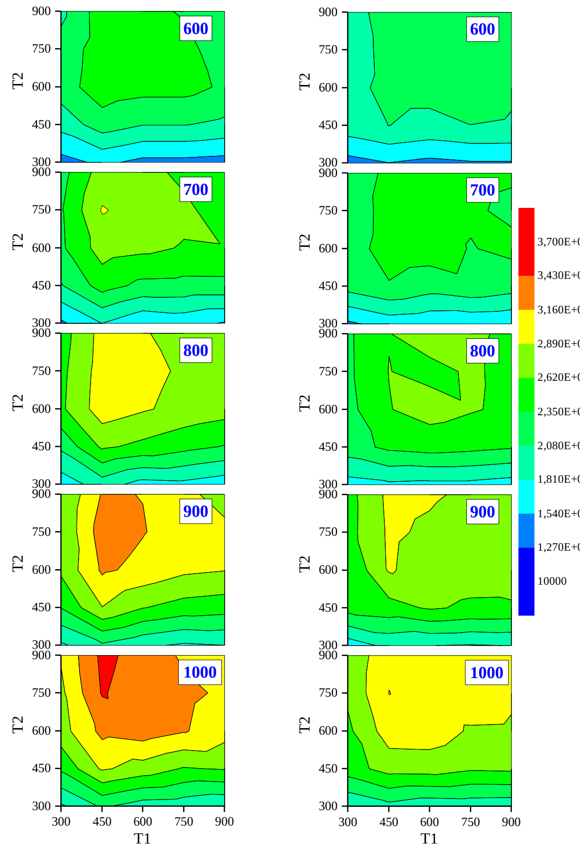

Fig. 1. Contour plots for effective detector gain dependence on transfer/induction gap voltages at fixed drift gap voltage of 500 V: (a) double conical and (b) cylindrical GEM holes.

Fig. 1 shows the obtained effective detector gain for two GEM hole geometries for $U_{drift} = 500\, V$. If one considers a single GEM foil, the gain will be higher when the electric field above the foil will not be high enough compared to field in the hole (making collection efficiency higher) *and* the field below the foil is high enough compared to field in the hole (making extraction efficiency higher). Projecting this onto three consecutive

GEM foils, in order to achieve the maximum gain one need to have the following situation with the electric fields: drift < T1 < T2 < induction. This situation is realized for both GEM detectors with double conical and cylindrical holes with such values: 1 kV/cm (500 V) < 2.25 kV/cm (450 V) < 3.75 kV/cm (750 V) < 5 kV/cm (1000 V). For the cylindrical holes the gain is somewhat smaller than for double-conical geometry. This is in agreement with [15] [16] where it was shown that the smaller inner diameter of the double-conical hole is better for collection and extraction efficiencies than bigger diameter of the cylindrical hole (i.e. smaller optical transparency is better). Therefore, higher ratio of external to hole electric fields is needed to reach the same efficiencies.

Therefore, an optimal electric field distribution allows maximizing the produced charge for each GEM hole geometry. Nevertheless, another factor that defines the final choice of the electric field distribution is relative energy resolution: it has to be maximized as well.

2.3 Energy resolution vs. electric field distributions

Statistical fluctuations of the primary electron number N as well as fluctuations of the detector amplification G broaden the impulse amplitude and, therefore, determine the maximal achievable energy resolution. Mathematically, the energy resolution of proportional counter is defined as: $\left(\frac{\sigma E}{E}\right)^2 = \left(\frac{\sigma N}{N}\right)^2 + \frac{1}{N}\cdot\left(\frac{\sigma G}{G}\right)^2 = \frac{(F+f)\cdot w_I}{h\nu}$, where σN and σG are the fluctuations of the primary electrons number and gas amplification, respectively. The first term is written through the Fano factor, F, that is constant characteristic to gases [17] ($\sim$0.19 for Argon [18]). The second term contains the variance of gas amplification for one electron $f = \sigma G/G$. It should be noted that a third term connected with the instrumentational error also exists. The stochastic nature of primary electrons creation and their subsequent amplification results in a distribution of total number of charge or electrons for a particular photon energy to have a Gaussian distribution. Then, the relative variance of gas amplification denotes the electron avalanche resolution, which is $\sim 0.6 - 0.7$ for Ar gas at $10^2 - 10^5$ electron multiplication [18], [19]. This worsen the spectral resolution of the detector by about $\sim$6% per GEM foil given its ultimate magnitude to be at the level of $\sim$20% for 5.9 keV photons.

In the above, it was assumed that recombination, electron attachment, space charge and photoelectric effects are negligible. An increase in the spread of the amplitude of the pulses can also be caused by structural imperfections, leading to a distortion in the distribution of the electric field distribution. Great influence on the energy resolution is provided by the stability of applied voltages and purity of the gas. Despite the fact that no attachment of electrons is observed for inert gases, CO_2, CH_4, etc., the presence of even insignificant amount (<0.1%) of electronegative molecules of H_2O, CO, O_2, C_2, etc., leads to significant deterioration of energy resolution, since the amplitude of the pulse becomes dependent on the location of the formation of the primary electrons. Additions of certain gases with an ionization potential that is lower than the ionization potential of the main gas component, can lead to a decrease in average energy spent on the formation of a pair of ions, hence to an improvement in resolution.

At high registration rates, an electron avalanche is weakened, as it is formed in the non-relaxed space charge from the previous avalanche. This attenuation is distributed according to a random law and causes not only a decrease in the amplitude of the pulses, but also worsens the energy resolution. At $\bar{G}\sim 10^4 - 10^5$ the highest counting rate is $10^5 - 10^6 s^{-1}$.

Fig. 2 contains the energy resolutions for two GEM hole geometries for different values of the induction and transfer voltages. It could be noticed that the double-conical detector shows both the best and the worst values for the resolution, whereas the cylindrical detector shows less variations.

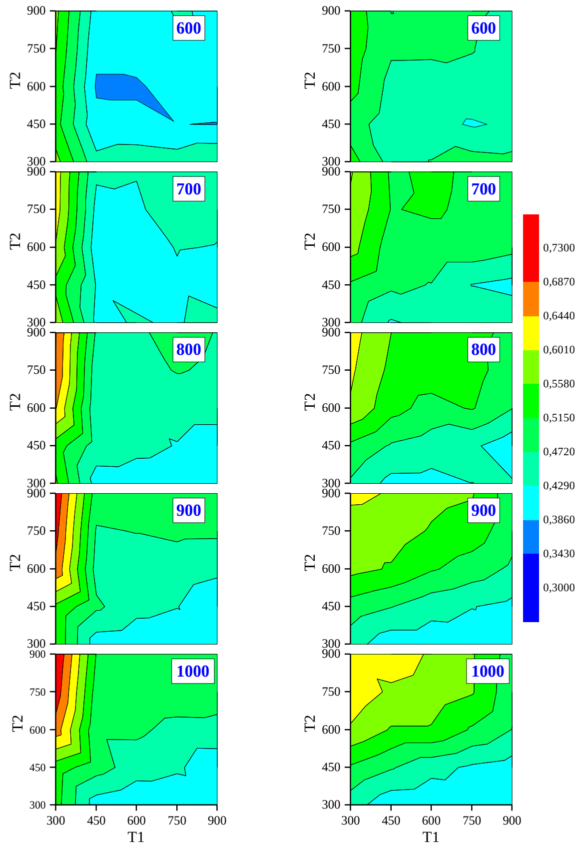

Fig. 2. Contour plots for energy resolution dependence on transfer/induction gap voltages at fixed drift gap voltage of 500 V: (a) double conical and (b) cylindrical GEM holes. Lower values mean better resolution.

In order to discuss the results qualitatively only, let us recall that for each GEM foil the collection and extraction efficiencies can be represented as functions of ratios between the corresponding external and hole electric fields [15]. At the same time, the electric field in a GEM hole can be approximated as a linear function of *sum* of external fields above and below the foil [15]. Using these approximations, mathematical expressions can be construed for gain and resolution for a triple GEM detector. It can be shown through cumbersome but straightforward calculations that the maximums of gain and resolution occur at different values of voltages (thorough analysis will be presented elsewhere). For the resolution the maximum is achieved when the electric fields of drift, transfer, and induction gaps are the same as opposed to the gain (see Section 2.2).

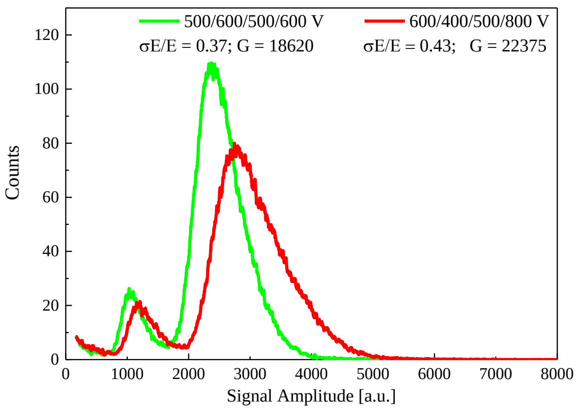

Fig. 3. Signal amplitude spectra collected for two sets of voltages applied to the detector’s gaps.

Fig. 3 shows an example of such situation. The gain is larger for set of voltages 600/400/500/800 V chosen to be an optimum within the simulation results presented in [20] with the electric fields following more or less the desired relationship mentioned in Section 2.2. Whereas, the resolution is better for the other set of voltages 500/600/500/600 V with the electric fields being very similar to each other. In this situation, optimal extraction and collection efficiencies result in better shape and linearity of the spectrum. Situation with the detector with cylindrical holes is similar but not as pronounced.

Developing a GEM based energy discrimination tomography at the tokamak would rather require the best achievable energy resolution than the highest gas amplification. This statement was also supported by the data presented in the next section.

2.4 Gain vs. photon flux intensity

A collimated ø1.2 mm beam of 8 keV photons from a copper X-ray tube (Cu K-line) without any additional monochromator was used to test the detector rate capability for both GEM holes configurations. The applied voltages in the drift, two transfer, and induction gaps were kept the same (1200/720/720/720 V), changing only the applied voltage on GEM foils. The rate of the photon absorption, mostly happening in the drift gap, was adjusted by modifying the intensity of the X-ray generator. The initial primary charge generated in the drift gap can be estimated knowing incident radiation energy (leading to an average of 290 generated primary electrons per event for Cu K-line photon) and the number of absorbed photons. Overall, the initial primary charge was estimated from the signals, event after event, from the bottom electrode of the last GEM. The results of the irradiation are presented in Fig. 4 for the gain as a function of the photon flux.

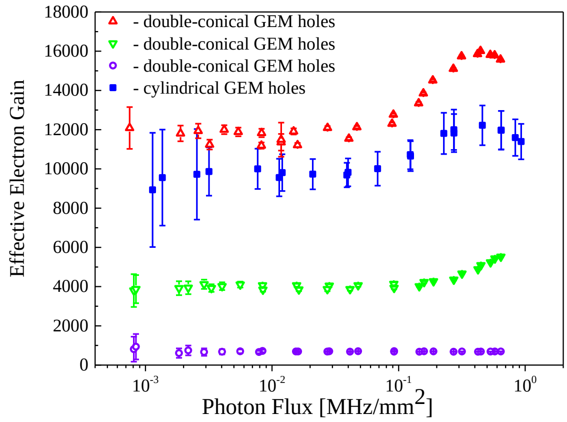

Fig. 4. Effective electron gain as a function of photon flux intensity for double-conical and cylindrical holes.

In case of double-conical holes, the effective gain was found to be stable in the wide range of the incident photon flux. High GEM voltage resulting in high detector gains, $\sim 10^4$, produces an almost constant effective gain up to $0.1 MHz/mm^2$ flux. Whereas decreasing the GEM voltage and, thus, gas amplification, extends the stable effective gain range significantly. At low gain of $\sim 10^3$, it stays constant up to almost $1 MHz/mm^2$. This behavior is strictly related to the space charge amount accumulated in the multiplication chain. For level of ion yield above ~ 20 (beyond $\sim 10^3 fC/cm^3$) [21] back drifting ions per incoming electron, the external electric field starts to distort considerably.

In case of cylindrical holes, the effective gain is also constant up to $0.1 MHz/mm^2$ and then rises but not as steep as in case of double-conical holes. Therefore, it might be more suitable for intense plasma radiation of high dynamics. In this case, a sudden growth of the photon flux over $0.1 MHz/mm^2$ is less dangerous for the detector, as the probability of discharges increases by almost an order for such gain change ($\sim 4 \cdot 10^3$ for double-conical holes) above the level of $\sim 10^4$ for $ArCO_2CF_4$ mixture [22], which has even better quenching properties than the investigated $ArCO_2$.

Considering the application of the detector for highly intense plasma radiation monitoring, it may be desired to operate the detector at as low as possible gas amplification to extend the stable operation range. Such working conditions would impose a serious requirement to be met by the dedicated electronics capabilities. Nevertheless, a compromise could be found to operate a detector at lower gains and still have a good signal-to-noise ratio.

3. Summary

A study of detector's performance (gain, resolution, and response under high photon flux) was undertaken for $ArCO_2$ filled detector. Two GEM hole shapes were examined within these tests. Control of electric field distribution affecting detector's amplification and spectral resolution was realized via selection of voltages at drift, two transfer, and induction gaps. Comparison of two different multiplier shapes allowed us to conclude that cylindrically shaped holes would provide more stable operation of the detector under plasma radiation environment and would be a good candidate for the final detector considering optimization of its spectral resolution.

Acknowledgments

This work has been carried out within the framework of the EUROfusion Consortium and has received funding from the Euratom research and training programme 2014-2018 under grant agreement No 633053. The views and opinions expressed herein do not necessarily reflect those of the European Commission. This work was partly supported by Polish Ministry of Science and Higher Education within the framework of the scientific financial resources in the years 2014-2017 allocated for the realization of the international co-financed project.

References

[1] F. Sauli, Development and applications of gas electron multiplier detectors, Nuclear Instruments and Methods in Physics Research A 505 (2003) 195-198.

[2] A. F. Buzulutskov, Radiation Detectors Based on Gas Electron Multipliers, Instruments and Experimental Techniques 50 (2007) 287–310.

[3] J. Rzadkiewicz et al., Design of T-GEM detectors for X-ray diagnostics on JET, Nuclear Instruments and Methods in Physics Research A 720 (2013) 36-38.

[4] M. Chernyshova et al., Development of GEM gas detectors for X-ray crystal spectrometry, Journal of Instrumentation 9 (2014) C03003.

[5] M. Chernyshova et al., Conceptual design and development of GEM based detecting system for tomographic tungsten focused transport monitoring, Journal of Instrumentation 10 (2015) P10022.

[6] T. Nakano et al., Determination of tungsten and molybdenum concentrations from an X-ray range spectrum in JET with the ITER-like wall configuration, Journal of Physics B 48 (2015) 144023.

[7] M. Chernyshova et al., Development of GEM detector for tokamak SXR tomography system: Preliminary laboratory tests, Fusion Engineering and Design (2017) in press.

[8] M. Chernyshova et al., Gaseous electron multiplier-based soft x-ray plasma diagnostics development: Preliminary tests at ASDEX Upgrade, Review of Scientific Instruments 87 (2016) 11E325.

[9] T. Czarski et al., The cluster charge identification in the GEM detector for fusion plasma imaging by soft X-ray diagnostics, Review of Scientific Instruments 87 (2016) 11E336.

[10] A. Wojenski et al., FPGA-based GEM detector signal acquisition for SXR spectroscopy system, Journal of Instrumentation 11 (2016) C11035.

[11] A. Wojenski et al., Concept and current status of data acquisition technique for GEM detector based SXR diagnostics, Fusion Science and Technology 69 (2016) 595-604.

[12] T. Czarski et al., Data processing for soft X-ray diagnostics based on GEM detector measurements for fusion plasma imaging, Nuclear Instruments and Methods in Physics Research B 364 (2015) 54-59.

[13] D. Mazon et al., Design of soft-X-ray tomographic system in WEST using GEM detectors, Fusion Engineering and Design 96-97 (2015) 856-860.

[14] A. Jardin et al., Tomographic capabilities of the new GEM based SXR diagnostic of WEST, Journal of Instrumentation 11 (2016) C07006.

[15] M. Killenberg et al., Modelling and Measurement of Charge Transfer in Multiple GEM Structures, Nuclear Instruments and Methods in Physics Research A 498 (2003) 369-383.

[16] O. Bouianov et al., Foil geometry effects on GEM characteristics, Nuclear Instruments and Methods in Physics Research A 458 (2001) 698-709.

[17] U. Fano, Ionization Yield of Radiations. 2. The Fluctuations of the Number of Ions, Physical Review 72 (1947) 26-29.

[18] G. D. Alkhazov, Statistics of electron avalanches and ultimate resolution of proportional counters, Nuclear Instruments and Methods 89 (1970) 155-165.

[19] G. D. Alkhazov, Mean value and variance of gas amplification in proportional counters, Nuclear Instruments and Methods 75 (1969) 161-162.

[20] M. Chernyshova et al., Development of GEM detector for plasma diagnostics application: simulations addressing optimization of its performance, Journal of Instrumentation (2017) in press.

[21] M. Ball et al., Ion backflow studies for the ALICE TPC upgrade with GEMs, Journal of Instrumentation 9 (2014) C04025.

[22] M. Alfonsi et al., A triple-GEM detector for high-rate particle triggering, Nuclear Instruments and Methods in Physics Research A 525 (2004) 17-19.